Baghdad Science Journal

Volume 23 | Issue 5 Article 22

5-29-2026

Semiautomated Online Continuous Flow Injection Analysis – Turbidimetric Determination of Zinc in Pharmaceutical Drugs

Raghad Saad Hatem
Department of Biology, College of Science, University of Kerbala, Kerbala, Iraq,
raghad.saad@uokerbala.edu.iq

Marwah A. Kadhim Al-Bana
Department of Forensic Science, College of Science, Al-Karkh University of Science, Baghdad, Iraq,
marwa.abd.alrada@kus.edu.iq

Nagham Shakir Turkey
Department of Chemistry, College of Science, University of Baghdad, Baghdad, Iraq,
nagamturkey@yahoo.com

Ihsan Mahdi Shaheed
Department of Chemistry, College of Science, University of Kerbala, Kerbala, Iraq,
Ihsan.aldahan@uokerbala.edu.iq

How to Cite this Article

Hatem, Raghad Saad; Al-Bana, Marwah A. Kadhim; Turkey, Nagham Shakir; and Shaheed, Ihsan Mahdi (2026) "Semiautomated Online Continuous Flow Injection Analysis – Turbidimetric Determination of Zinc in Pharmaceutical Drugs," *Baghdad Science Journal*: Vol. 23: Iss. 5, Article 22.
DOI: https://doi.org/10.21123/2411-7986.5306

BAGHDAD SCIENCE JOURNAL 2026;23(5):1852–1867

Scan the QR to view the full-text article on the journal website

RESEARCH ARTICLE

Semiautomated Online Continuous Flow Injection Analysis – Turbidimetric Determination of Zinc in Pharmaceutical Drugs

Raghad Saad Hatem [1], **Marwah A. Kadhim Al-Bana** [2], **Nagham Shakir Turkey** [3], **Ihsan Mahdi Shaheed** [4,*]

[1] Department of Biology, College of Science, University of Kerbala, Kerbala, Iraq
[2] Department of Forensic Science, College of Science, Al-Karkh University of Science, Baghdad, Iraq
[3] Department of Chemistry, College of Science, University of Baghdad, Baghdad, Iraq
[4] Department of Chemistry, College of Science, University of Kerbala, Kerbala, Iraq

ABSTRACT

This study has assessed the novel technology developed for our in-house NAG-5SX1-1D-SSP analyzer by utilizing the established reaction of the zinc (II) ion with ammonium thiocyanate and mercury (II) chloride to produce a white precipitate. This analyzer was used to access turbidity by calculating the reflection of incident light. The method maintains linear behavior over a concentration range from 0.05 to 18 mmol. L^{-1}, with a detection limit of 0. 489μg.sample^{-1} and excellent precision (RSD% >1). These results confirmed the reliability and robustness of the developed instrument for Zn (II) determination in various pharmaceutical formulations. Successful detection of Zn (II) ion was achieved in three drug formulations by using the standard addition approach. A comparative analysis was conducted between the newly devised approach and the conventional method (UV-Vis spectrophotometer) at a wavelength of 227 nm through the implementation of an individual and paired t-test. The data obtained underwent rigorous mathematical treatment, revealing no significant variance between the two methodologies in the analysis of three distinct drugs at a 95% confidence level.

Keywords: Flow injection analysis, Zinc (II) ion, Turbidity, Mercury (II) ammonium thiocyanate, Pharmaceutical analysis

Introduction

Zinc is considered one of the most important chemical elements in the human body, the largest percentage found in addition to other organs containing different percentages, such as the liver, kidneys, lungs, gastrointestinal tract, prostate, heart, and pancreas.[1] Sufficient availability of zinc is of particular importance to the immune system.[2] Thereby, it plays a key role in multisided cellular and molecular mechanisms. For instance, zinc influences the lymphocyte response to mitogens and cytokines, serves as a cofactor for the thymic hormone thymulin, and is involved in leukocyte signal transduction.[3] Due to its particular biological importance, fast and accurate analytical techniques for the determination of zinc are required, of which electrochemical,[4,5] spectrophotometry,[6] atomic absorption spectrometry,[7] and continuous flow analysis are the most commonly used.[8,9] Flow injection analysis has the advantage of being an automated technique with numerous and widespread applications in quantitative chemical[10] analysis, especially in pharmaceutical analysis.[11,12] In brief, a flow system involves the injection of a defined volume of sample into a moving stream of

Received 24 May 2025; revised 14 December 2025; accepted 2 January 2026.
Available online 29 May 2026

* Corresponding author.
E-mail addresses: raghad.saad@uokerbala.edu.iq (R. S. Hatem), marwa.abd.alrada@kus.edu.iq (M. A. K. Al-Bana), nagamturkey@yahoo.com (N. S. Turkey), ihsan.aldahan@uokerbala.edu.iq (I. M. Shaheed).

https://doi.org/10.21123/2411-7986.5306

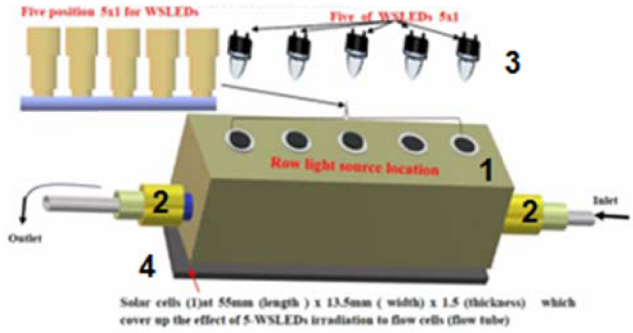

Fig. 1. 3D-representation of the metal block incubator of five successive LEDs, flow cell.

a solution, which serves as a carrier that flows the sample through a detector. Between the injection and detection points, the sample of interest is physically or chemically transformed into a detectable species. Flow injection is generally a very fast, simple, and inexpensive technique, employing common instrumentation. Compared to batch analytical methods, it offers increased sampling frequency, low expense of reagents and samples, and increased precision and high sensitivity.[13–15] There is a dearth of research on the coupling of continuous flow injection with turbidity measurements.[16,17] In this research, the proposed method and the NAG-5SX1-1D-SSP analyzer incorporate several key innovations and advantages, including a novel detection principle in which turbidity is detected by reflected scattered incident light over an angular range from 0 to 180 degrees, enabling more extensive signal collection than traditional single-single detectors. The modified design of the analyzer combines a quartz flow cell, several LED light sources, and a solar cell detector to provide a simple yet highly efficient analytical performance. The system exhibited excellent precision and sensitivity, achieving a low detection limit (LOD) of 0. 489μg.sample-1 and an excellent (RSD% >1), which confirms excellent repeatability and analytical reliability. In addition to that, the analytical response maintains a wide concentration range of 0.05–18 mmol. L^{-1}, making the proposed method suitable for pharmaceutical formulation containing Zn (II) ion at different levels. The analyzer is suitable for routine quality control due to its compact size, cost-effectiveness, and lack of the need for complex optics or highly trained workers. Successful validation was maintained by utilizing a comparative study with UV-visible spectrophotometry, which revealed no statistically significant difference at the 95% confidence level, confirming the accuracy of the new method.

Materials and methods

Chemicals

Ammonium thiocyanate (NH_4SCN) (Fluka). Mercury (II) chloride ($HgCl_2$) (BDH). Zinc sulfate heptahydrate (BDH). CH_3COOH (BDH). Sulfuric acid (BDH). HCl (BDH). HNO_3 (BDH). H_3PO_4 (BDH).

Apparatus

The main measuring unit of the NAG-SSP analyzer is composed of four distinct parts, as shown in Fig. 1.

1- The metal incubator: this is composed of brass metal that has faces of 40 mm x 40 mm with a 55 mm length; therefore, it will have four side faces. Each side face is 40 mm x 55 mm, two of which face each other; one of these will be used to mount the irradiation sources, the snow-white LEDs.
2- Flow cell: All the turbidimetric measurements were carried out using a flow cell. This cell is made of quartz and has a full length of 105 mm, and is composed of two parts that form a single piece, each being 55 mm in length.
3- Sources side: The range of the visible region was covered by using five LEDs, as shown in Fig. 2. The irradiation sources consisted of five LEDs (diameter 10 mm, height 10 mm, rim 11 mm $\times$ 1 mm) operated at 0–3.6 V DC. The emission spectrum covered three distinct bands: blue (460 nm), green (523 nm), and red (622 nm).
4- A single solar cell used as a direct optical detector.

The NAG-5SX1-1D-SSP analyzer offers a number of significant performance enhancements over traditional detectors. Five highly efficient snow-white LEDs are used to generate stable light output, minimal baseline deviation, and excellent spectral and thermal stability. High sensitivity has been maintained

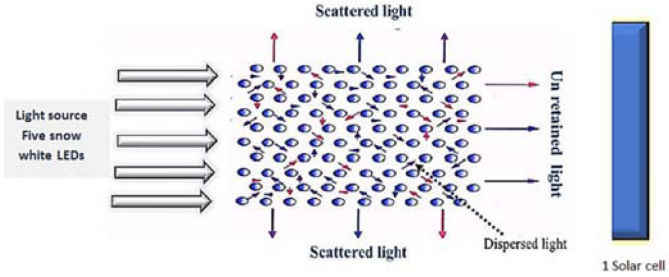

Fig. 2. Possible reflection and refraction inside and outside particles by the light source used.

due to the combination of a quartz flow cell with 0–180 degree scattering angle detection, resulting in a low detection limit of 0.489 μg. sampl^{-1}. The homemade device is less expensive than a UV-Vis spectrophotometer since it uses frequently accessible components (solar-cell detector, LEDs, and brass housing) and its compact size (40×40×55 mm) allows for easy transportation. Electronic noise is eliminated without the use of an electronic filter, leading to improved signal quality. A novel variable-diameter tubing design (1–4mm) reduces turbulence and enhances sensitivity by acting as a hydraulic shock absorber, leading to increased precipitate packing and turbidity intensity. Additionally, the system offers variable–flow rate control, adjustable light intensity (0–3.6V), and good intra-day and inter-day repeatability.

Overall, the NAG SSP analyzer can be considered a well-suited choice for pharmaceutical quality control since it is a sensitive, dependable, affordable, and portable instrument with optimal noise suppression.

A manifold flow injection system, which consists of a three-channel peristaltic pump (Ismatic type ISM796 from Switzerland), was used to transport the carrier solutions. A rotary six-port medium-pressure injection valve made of Teflon, manufactured by INDEX Corporation, USA, is used to provide appropriate injection volumes of standard solutions and samples.

The NAG-SSP analyzer was first designed and constructed in our laboratory. Its operating principle relies on turbidimetric detection within a brass incubator block (55 × 40 × 40 mm) housing a quartz flow cell (105 mm total length). Irradiation is provided by five snow-white LEDs mounted on one face, while detection is achieved by a single 55 mm solar cell mounted opposite the sources. The use of a single solar cell eliminates voltage loss associated with multi-cell configurations, thereby enhancing stability and reproducibility.

For comparison purposes, Zn (II) ion determination was also performed using a Shimadzu UV-1800 UV-Vis spectrophotometer (Shimadzu Corporation, Kyoto, Japan). Measurements of absorbance were performed at a maximum wavelength (λ227) using 1cm quartz cell. The instrument was calibrated against reagent blanks, and baseline correction was applied to ensure accuracy and reproducibility.

Preparation of reagents

Ammonium thiocyanate (NH_4SCN) solution

0.10 mol.L^{-1} (76.122 g.mol^{-1}, Fluka purity ≥ 99%). Dissolve 7.6122 g.1^{-1} L of water.

Mercury (II) chloride ($HgCl_2$) solution

0.05 mol.L^{-1} (271.52 g.mol^{-1}, BDH purity ≥ 99%). Dissolve 13.9 g in water and make up the solution to 1 L.

Zinc sulfate heptahydrate solution

50 mmol (287.53g.mol^{-1}, BDH purity ≥ 98%). Dissolve 3.5941 g.250 mL^{-1}

CH_3COOH solution

1.00 mol.L^{-1} (BDH, purity 99.5%). Dilute 28.7 mL of 99.5% CH_3COOH (specific gravity 1.05) with distilled water in a 500 mL flask. Standardized with NaOH solution.

Sulfuric acid solution

1.00 mol. L^{-1} (BDH, purity 96%). Dilute 27.8 mL of 96% H_2SO_4 (specific gravity 1.84) with distilled water in a 500 mL flask. Standardized with Na_2CO_3 solution.

HCl solution

1.00 mol. L^{-1} (BDH, purity 35%). Dilute 44.95 mL of 35% HCl (specific gravity 1.16) with distilled water in a 500 mL flask. Standardized with Na_2CO_3 solution.

HNO_3 solution

1.00 mol. L^{-1} (BDH, purity 70%). Dilute 31.69 mL of 70% HNO_3 (specific gravity 1.42) with distilled water in a 500 mL flask. Standardized with Na_2CO_3 solution.

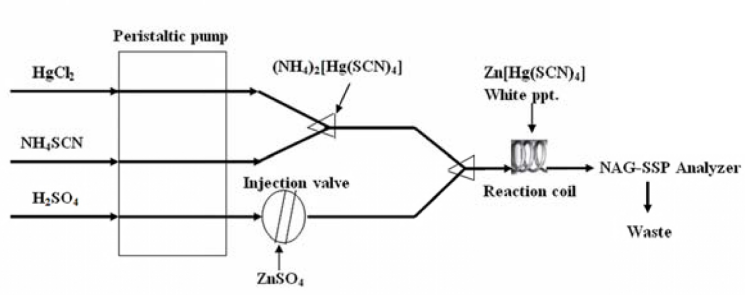

Fig. 3. NAG-SSP analyzer coupled with three lines of the flow injection system used for the determination of zinc (II) ions.

H_3PO_4 solution

1.00 mol. L^{-1} (BDH, purity 85%). Dilute 33.92 mL of 85% phosphoric acid (specific gravity 1.7) with distilled water in a 500 mL flask. Standardized with Na_2CO_3 solution.

All experiments involving mercuric chloride were conducted inside certified fume hoods. Researchers wore appropriate personal protective equipment (PPE), including nitrile gloves, protective eyewear, and lab coats, to minimize exposure risk. Mercury – containing solutions were prevented from entering routine laboratory drains and were stored in chemically resistant containers. The accumulating waste was chemically treated with sulfide reagent, which converted soluble mercury ions into their insoluble form (HgS), leading to a reduction in toxicity. The validated protocol confirms that the proposed method is scientifically robust and environmentally sustainable, making it appropriate for routine application in pharmaceutical quality control. All experiments were performed in complete accordance with applicable local and international safety frameworks established by the World Health Organization (WHO) and the Environmental Protection Agency (EPA). The validated protocol states that the proposed method meets scientific and environmental safety standards for routine quality control.

Preparation of the sample

Three commercial formulations were investigated as sources for Zn (II) ions in this study: Zinc tablet 20 mg (Pharma Development, France), Wellzinc 20 mg (Wellona Pharma, India), and zinc tablet 20 mg (Coral Lab., India). The zinc sulfate tablet solution procedure involves carefully weighing and finely pulverizing 20 tablets of each commercial medicine, with each tablet containing 20 mg of zinc sulfate in its monohydrate form. This was conducted to ascertain the concentration, which was 0.5 mmol. L^{-1}. A specific quantity of each of the powdered tablet types (0.02989 g, 0.0348 g, and 0.0203 g, respectively), equivalent to 54.901 mg of the active component zinc ion in each case, from the above brands, was transferred into a beaker and dissolved in distilled water using a stirrer. Once the solutions had been filtered to remove any residual undissolved components, the residue was washed three times and then made up to a final volume of 100 mL using distilled water.

Analytical procedure

Zinc (II) ion assessment was based on the use of two reagents: ammonium thiocyanate and mercury (II) chloride. The two reagents react with each other continuously within the flow system to form a precipitate, mercury (II) ammonium thiocyanate, $(NH_4)_2[Hg(SCN)_4]$, which reacts with the injected zinc (II) ion sample to form a white precipitate, $Zn[Hg(SCN)_4]$. Fig. 3 shows the three-line manifold designed to carry out this research. The first line contains sulfuric acid (7.00 mmol.L^{-1}) as a carrier for the zinc sulphate sample (7.00 mmol.L^{-1}, 170 μL sample volume), while the second and third lines contain the two reagents that form the precipitating agent, NH_4SCN (0.05 mmol.L^{-1}) and $HgCl_2$ (0.03 mmol.L^{-1}). All three lines are run at the same flow rate of 1.3 mL.min^{-1}. The zinc (II) ions encounter the precipitating agent at the second Y-junction point, and then enter the reaction coil (50 μL) to complete the precipitation process. The white precipitate so formed passes into the flow cell of the NAG-SSP analyzer.

Results and discussion

The NAG-SSP instrument was used to examine various chemical and physical factors with the aim of determining the optimal parameters for use in subsequent experiments. The optimization process involved the use of a single variable mode while systematically varying a single parameter at a time, and additionally, the use of the slope-intercept method. The use of the slope-intercept method, as adopted

Table 1. Experimental variables selected for use in subsequent studies.

Physical and chemical parameters	
Sample volume (μL)	150
Flow rate of three lines (mL.min^{-1})	1.50
Carrier stream	H_2O
$HgCl_2$ concentration(mmol. L^{-1})	0.01
$ZnSO_4.7H_2O$ (mmol. L^{-1})	7.00
Without reaction coil	

previously.[18,19] It shows that it can be used for optimization of a state in which it is difficult to decide the optimum value. Thus, in the slope-intersection method, several segments can be drawn in an associated graph, where each segment consists of two, three, or four points; the optimal segment is selected based on the greatest intercept, which is a measure of sensitivity, and the lowest gradient in order to obtain the largest number of points for the studied variable. Each measurement output is repeated three times. All parameters used are tabulated in Table 1.

Effect of ammonium thiocyanate concentration on precipitate formation

Different concentrations of ammonium thiocyanate (reagent no. 1) in the concentration range 0.01–0.10 mmol. L^{-1} were used to study the effects of variation in NH_4SCN on the formation of the white precipitate. From Table 2 and Fig. 4, it was noted that lower concentrations might not be sufficient to allow the precipitation process to go to completion (i.e., <0.05 mmol. L^{-1}), while higher concentrations (i.e., >0.05 mmol. L^{-1}) might result in a decrease in sensitivity due to an increase in the agglomeration of the white precipitate and thus a decrease in the height of the response. Therefore, the optimal concentration was selected as 0.05 mmol. L^{-1}. From the slope–intercept method, it may be noted that the chosen optimal concentration falls within the two segments, and the S2 segment that extends from 0.05–0.10 mmol. L^{-1}represents a high sensitivity. Thus, 0.05 mmol. L^{-1} was selected as the optimal concentration.

Effect of mercury (II) chloride concentration on precipitate formation

After choosing the optimal concentration of NH_4SCN, a series of $HgCl_2$ solutions (0.005–0.100 mmol.L^{-1}) were prepared to select the optimum concentration for continuous mixing with ammonium thiocyanate. This, in turn, would form the mercury (II) ammonium thiocyanate that would be used to precipitate the zinc (II) ion as a white precipitate. From Table 3 and Fig. 5, it was noticed that the recorded response increased with increasing $HgCl_2$ concentration up to 0.03 mmol.L^{-1}. Past this, increasing the mercury (II) chloride concentration further led to a decrease in the amount of light reaching the single solar cell. Segment S2, at a concentration of 0.03 mmol.L^{-1} (slope-intercept method), was chosen as it is the most sensitive according to the value of the associated intercept (a). Therefore, 0.03 mmol.L^{-1} was chosen as the optimum concentration.

Effect of the type of media as the carrier stream on the formation of the Zn[Hg(SCN)$_4$] precipitate

The reaction system, NH_4SCN-$HgCl_2$-$ZnSO_4$, used to form the white precipitate was studied in different acidic media (CH_3COOH, H_2SO_4, HNO_3, HCl, and H_3PO_4) at concentrations of 10 mmol.L^{-1}, in addition to H_2O, as the carrier streams. The type of carrier stream may affect the precipitation process, speed of precipitate particle formation, the purity of the precipitate, and whether nuclei grow to form larger particulates or otherwise dissociate. From Table 4 and Fig. 6, it was noted that sulfuric acid with distilled water as the carrier stream showed the best response because it gave sharp, intense peak profiles compared with other acids. This can be attributed to the other acids' ability to break up the precipitate, which would not then attenuate the incident light. Therefore, H_2SO_4 was considered the best medium for use in the reaction system.

Effect of H_2SO_4 concentration in the carrier stream on output response of the NAG-5SX1-1D-SSP instrument

H_2SO_4 solution was found to be the most effective medium for the precipitation process and in increasing the intensity of the response obtained, as described above. This might well be attributed to an increase in the agglomeration of the white precipitate capable of attenuating the light incident on the solar cell. On this basis, sulfuric acid was used as the carrier stream to carry zinc ions, to improve the sensitivity of any measurements. A number of sulfuric acid solutions were prepared, ranging from 3 to 15 mmol.L^{-1} .The responses and results of such are presented in Fig. 7 and Table 5, which show that, at concentrations greater than 7.00 mmol.L $^{-1}$ there is a decrease in recorded response due to an increase in the solubility of $Zn[Hg(SCN)_4]$ and formation of only small particles. Depending on the slope-intercept method, the optimal segment (S2) includes the optimal concentration of H_2SO_4, 7.00 mmol.L^{-1}, which was then used for subsequent experiments.

Table 2. Variation of ammonium thiocyanate concentration with output of response and segmentation mode (sample size 150μL, flow rate1.5mL.min^{-1} with distilled water as a carrier stream).

[SCN$^-$]mmol.L^{-1}	Output of response $\bar{y}$i (n = 3)(mV)	Standard deviation(SD)	Relative standard deviation (RSD%)
0.01	200	0.637	0.31
0.03	350	0.599	0.17
0.05	488	0.737	0.15
0.07	340	0.794	0.23
0.10	150	0.786	0.52
	Segmentation mode		
Segment	[SCN-] range mmol.L^{-1}	b (slope) (mV.mM^{-1})	a (Intercept) (mV)	Correlation (r)
S1	0.01–0.05	7200	130	0.9997
S2	0.05–0.10	–6726.32	819.26	0.9990

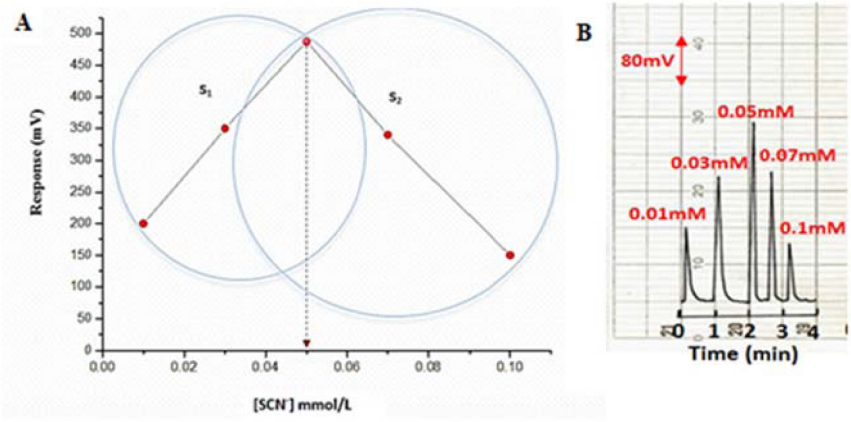

Fig. 4. Variation of ammonium thiocyanate concentration with: A-instrument response (mV). B-recorded NAG-SSP analyzer signal.

Table 3. Effect of variation of mercury (II) chloride concentration on white precipitate formation (sample size 150μL, flow rate1.5mL.min^{-1} with distilled water as a carrier stream).

[$HgCl_2$]mmol.L^{-1}	Output of response $\bar{y}$i (n = 3) (mV)	Standard deviation (SD)	Relative standard deviation (RSD%)
0.005	220	0.906	0.41
0.008	333	0.637	0.19
0.01	488	0.597	0.12
0.03	535	0.499	0.093
0.05	440	0.536	0.12
0.07	328	0.818	0.25
0.10	210	0.859	0.41
	Segmentation mode		
Segment	[$HgCl_2$] range mmol.L^{-1}	b (mV/mM)	a (mV)	Correlation (r)
S1	0.005–0.01	52342.11	–54.29	0.9790
S2	0.03–0.07	–5175.00	693.08	0.9989
S3	0.05–0.10	–4547.37	659.47	0.9950

Effect of flow rate

Flow rate plays an important role in flow injection techniques, especially when the precipitation process occurs in the flow system, as this can influence the sensitivity. Conversely, reduced injection rates may result in well clogging, altering hydraulic conductivity, and necessitating a comprehensive understanding of clogging factors to optimize system design. A thorough comprehension of the correlation between flow rate and system reactions is imperative for precise interpretation. On this basis, using the same optimized

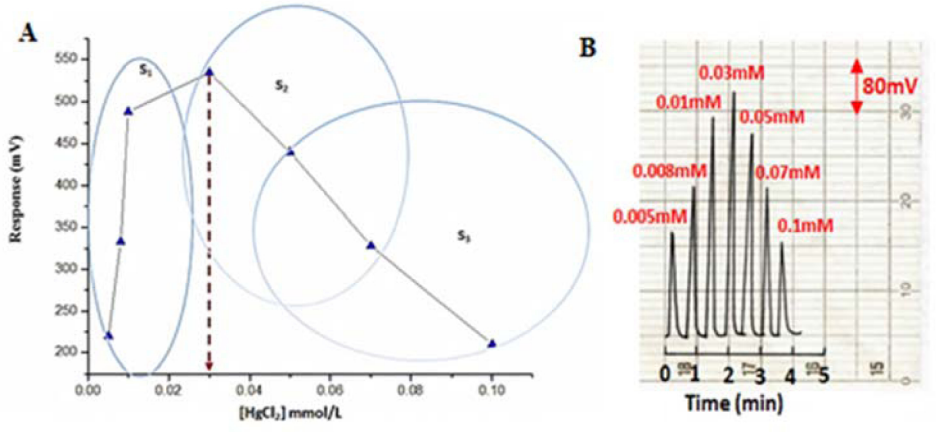

Fig. 5. A- Plot of average output response versus $HgCl_2$ concentration. B- Recorded response of Zn(II) ion with change in concentration of $HgCl_2$.

Table 4. Effect of using different acids as carrier streams on white precipitate formation using 0.05mmol. $L^{-1}NH_4SCN$-0. 03mmol.$L^{-1}HgCl_2$-7mmol.L^{-1} $ZnSO_4$ system with sample size 150μL and flow rate1.5mL.min^{-1}.

Type of media as a carrier stream $[H_3O^+]$ 10 mmol.L^{-1}	Output of response $\bar{y}i$ (n = 3) (mV)	Standard deviation (SD)	Relative standard deviation (RSD%)
H_2O	535	0.798	0.15
CH_3COOH	545	0.814	0.15
H_2SO_4	635	0.737	0.12
HNO_3	510	0.738	0.15
HCl	490	0.704	0.14
H_3PO_4	348	0.677	0.195

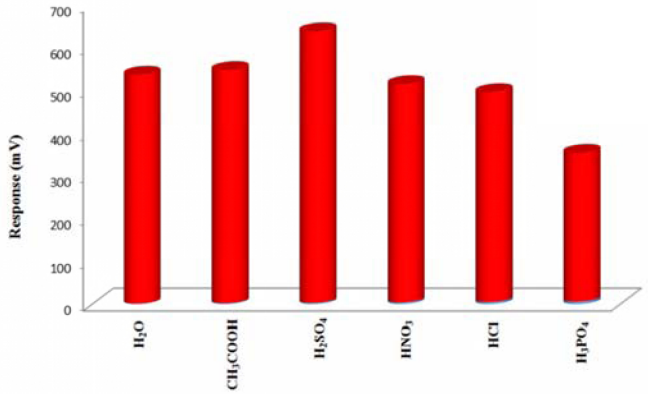

Fig. 6. Effect of type of carrier stream as a column representation of the contribution of each media.

parameters as in the above studies, variable flow rates in the range 0.8–2.0 mL.min^{-1} were used. The results so obtained are reported in Fig. 8 and Table 6, from which it may be noticed at a low flow rate increased the dispersion effect on the $Zn[Hg(SCN)_4]$ precipitate segment and increased the segment area of white precipitate in the flow cell up to 1.3 mL.min^{-1}, past which (i.e., >1.3 mL.min^{-1}) there was a significant decrease in the recorded response; this latter effect might be attributed to incomplete formation of the precipitating reagent, leading to a decrease in the amount of $Zn[Hg(SCN)_4]$ particulates. On this basis, the optimum flow rate was selected to be 1.3 mL.min^{-1} to produce highly sensitive, precise, and constant recorded signals.

Study of the optimum sample volume used in the NH_4SCN-$HgCl_2$-$ZnSO_4$ system

The effect of sample volume (7.00 mmol.L^{-1} Zn(II) ion) was studied using various volumes of $ZnSO_4$ in the range 50–200 μL by changing the length of the

Table 5. Summary of the results obtained and the application of the slope-intercept method (Sample size 150μL, flow rate1.5mL.min^{-1}).

$[H_2SO_4]$mmol.L^{-1}	Output of response $\bar{y}i$ (n = 3)(mV)	Standard deviation(SD)	Relative standard deviation (RSD%)
3	584	0.737	0.13
5	620	0.800	0.13
7	688	0.778	0.11
10	**635**	0.734	0.12
13	554	0.718	0.13
15	483	0.857	0.18
	Segmentation mode		
Segment	$[H_2SO_4]$ range mmol.L^{-1}	b (mV/mM)	a (mV)	Correlation (r)
S1	3–10	8.38	579.36	0.5797
S2	7–15	–25.49	876.84	0.9901

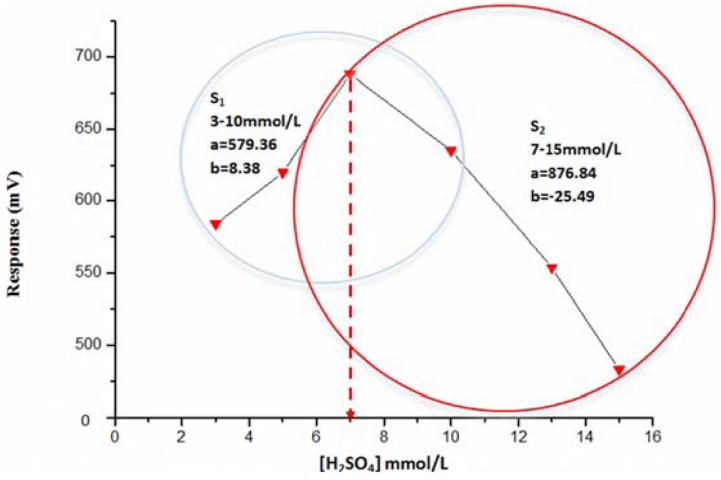

Fig. 7. Effect of variable concentration of H_2SO_4 solution on the output of the response.

Table 6. Effect of flow rate on $Zn[Hg(SCN)_4]$ precipitate formation using the NAG-SSP.

Flow rate for three lines mL.min^{-1}	Output of response $\bar{y}i$ (n = 3) (mV)	Standard deviation (SD)	Relative standard deviation (RSD%)
0.8	510	0.858	0.17
1.0	632	0.826	0.13
1.3	755	0.782	0.10
1.5	688	0.769	0.11
1.7	439	0.718	0.16
1.9	400	0.775	0.19
2.0	358	0.794	0.22

loop in the injection valve. It was recognized from Table 7 and Fig. 9 that the most suitable volume of $ZnSO_4$ was 170 μL, which gave sharp maximum peaks, regularly recorded signals, and a decreased peak base width. Volumes greater than 170 μL led to reduced peak intensity with distortion of the signal recorded and an increase in peak base width. This was attributed to a high density of $Zn[Hg(SCN)_4]$ precipitate, where extensive precipitate formation will enhance the internal filtering effect of the precipitate on the incident light intensity, as well as the divergent light intensity. For the above reasons, 170 μL was chosen as the optimum sample volume, which falls within the S3 segment (170–200 μL), with its large intercept and high sensitivity.

Effect of reaction coil

One of the aims of this study was to decide whether the precipitation reaction requires a reaction coil to complete the formation of the white precipitate, and

Table 7. Effect of the variation of Zn(II) ion on formation of the $Zn[Hg(SCN)_4]$ precipitate, as calculated via the slope-intercept mode. (flow rate1.3mL.min^{-1} with 7mmol.L^{-1} H_2SO_4 as carrier stream).

Volume of Zn(II) segment (μL)	Output of response $\bar{y}$i (n = 3)(mV)	Standard deviation (SD)	Relative standard deviation (RSD%)
50	322	0.701	0.22
70	400	0.802	0.20
90	495	0.794	0.16
100	573	0.697	0.12
130	647	0.734	0.11
150	755	0.798	0.11
170	798	0.818	0.10
190	703	1.200	0.17
200	610	1.394	0.23

Segmentation mode				
Segment	Volume of segment Range μL	b (mV/mM)	a (mV)	Correlation (r)
S1	50–90	4.33	102.92	0.9984
S2	100–150	3.55	209.00	0.9754
S3	170–200	–6.05	1833.00	0.9831

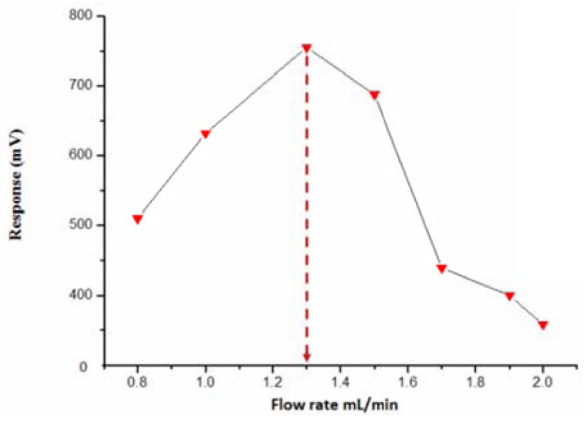

Fig. 8. Effect of variation in flow rate on $Zn[Hg(SCN)_4]$ precipitate formation using the NAG-SSP analyzer.

further whether there would be sufficient time to grow and form granules (which increase the sensitivity by repeated homogenization of precipitate particulates) or otherwise by the direct attachment of such to the flow system. Thus, a variable length of delay reaction coil (without coil – 200 μL) was connected between the second junction point and the flow cell. It may be noted from Table 8 that there was an increase in the signals recorded by the NAG-SSP analyzer when using a delay reaction coil equivalent to 50 μL, above which a decrease in signal was obtained with a notable distortion in the shapes of the associated peaks. This might be attributed to diffusion and dispersion factors associated with the white precipitate particulate segment due to increases in dispersed regions that mostly led to the accumulation of precipitate particles, reducing the reflecting surface. Thus, a 50 μL reaction coil was used to complete the formation of the $Zn[Hg(SCN)_4]$ precipitate, in complete agreement with the slope-intercept method as explained in Fig. 10, which shows that the first segment (S1:50–150 μL) is optimal, as based on obtaining comparable sensitivity results to S2.

Studying calibration curve, repeatability, and detection limit for the developed and classical methods

Using the optimum chemical and physical parameters, a series of Zn(II) ion solutions ranging from 0.05–20 mmol.L^{-1} in concentration were prepared. Table 9 tabulates the calibration curve for the instrument response of the NAG-SSP analyzer. Figs. 11 and 12 show a scatter plot diagram. A calibration graph was derived from the scatter plot encompassing the range 0.05–20 mmol. L^{-1}, exhibiting a correlation coefficient of r = 0.9963. The linear plot extended from 0.05–18 mmol. L^{-1} with a correlation coefficient r = 0.9992. All associated findings are summarized in Table 9. The NAG-SSP instrument was compared with a UV-Vis spectrophotometer with regard to the determination of the Zn(II) ion, the method for which is based on UV-spectroscopic measurements at λmax= 227 nm as shown in Figs. 13 and 14. This method involves measuring absorbance within the range 0.008–3.70 mmol.L^{-1}, utilizing a quartz cell. Analysis of the scatter plot indicates that the optimal linear range for Zn(II) ion lies between 0.008–3.50 mmol.L^{-1}, exhibiting a correlation coefficient of 0.9975 and an R_2 = 99.50%. Repeatability was evaluated at two representative concentrations: 9.00 mmol·L^{-1} (lower concentration example) and 16.00 mmol·L^{-1} [1] (higher concentration example)

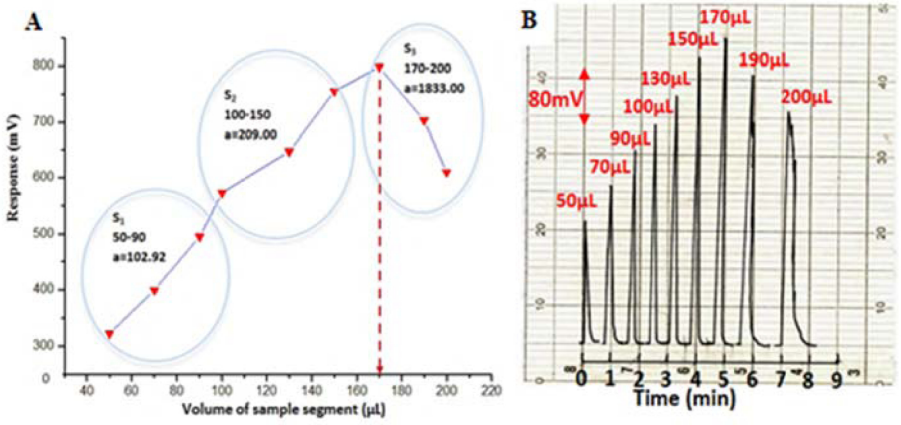

Fig. 9. A-Effect of the variation of Zn(II) ion on the formation of the $Zn[Hg(SCN)_4]$ precipitate B-Signal recorded using the NAG-SSP analyzer.

Table 8. Effect of the use of a delay reaction coil on the formation of the $Zn[Hg(SCN)_4]$ precipitate with the calculation of slope-intercept mode using optimum sample size 170μL and flow rate 1.3mL.min^{-1}.

Volume of reaction coil and formation of white precipitate (μL)	Output of response $\bar{y}$i (n = 3) (mV)	Standard deviation (SD)	Relative standard deviation (RSD%)	Segmentation mode
Without reaction coil	798	0.499	0.06	S1
				50–150 μL
50	845	0.794	0.09	a = 901.30
				b = –1.570
				r = 0.8983
100	700	0.762	0.11	
150	688	0.999	0.15	S2
				100–200 μL
200	450	1.259	0.28	a = 987.70
				b = –2.500
				r = 0.8865

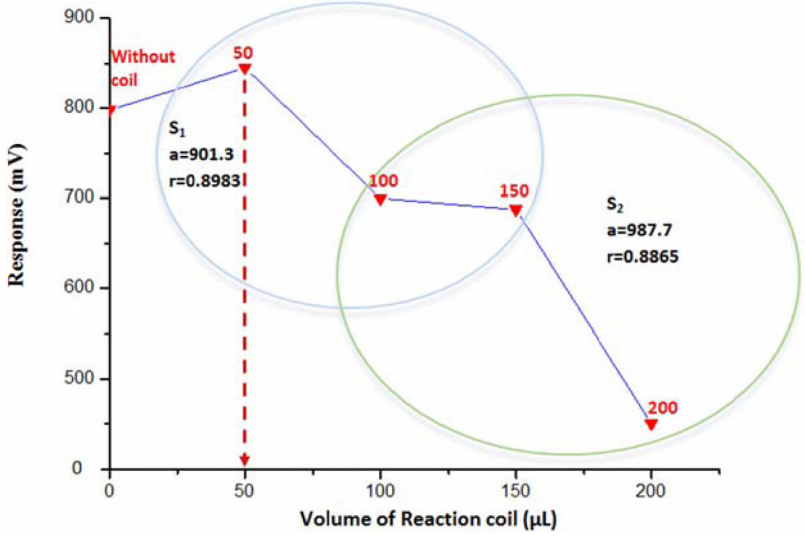

Fig. 10. Effect of reaction coil on formation of $Zn[Hg(SCN)_4]$ precipitate.

(Fig. 15). These points were selected to demonstrate the precision of the NAG-SSP analyzer across different regions of the calibration curve. In both cases, the relative standard deviation was less than 0.5%, confirming the robustness and reproducibility of the method, while for the classical method, the

Table 9. Analytical parameters, scatter, and calibration equation for the NAG-SSP instrument.

				Detection limit	Repeatability n=6	
Type of mode of range concentration	Range of concentration of Zn(II) mmol.L^{-1}	$\hat{Y}$(mV) = a ± SD + b ± SD[x] mmol.L^{-1}	r r2 R_2 %	Gradual dilution of the minimum concentration	Concentration mmol.L^{-1}	RSD%
Scatter plot	0.05–20 (n=19)	55.29 ± 25.31 + 102.88 ± 2.16 [Zn(II)] mmol.L^{-1}	0.9963 0.9926 99.26%	(0.01 mmol.L^{-1}) 0.489 μg/μL	9	0.234
Linear range	0.05–18 (n=17)	36.55 ± 11.79 + 107.27 ± 1.13 [Zn(II)] mmol.L^{-1}	0.9992 0.9983 99.83%		16	0.523

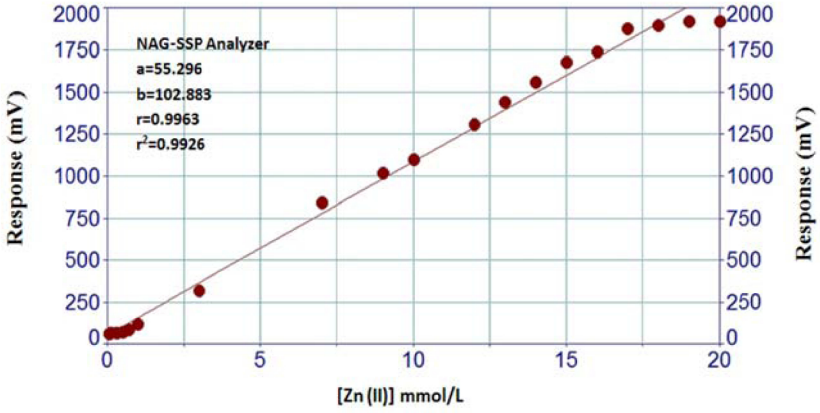

Fig. 11. Scatter plots of variable range concentrations showing the relation between the concentration of Zn(II) and signal response for the NAG-SSP analyzer.

repeatability for 0.01 and 3.00 mmol.L^{-1} was RSD% $<0.5\%$. All results are summarized in Tables 9 and 10.

The continuous flow injection analysis via turbidimetric measurements using the NAG-SSP analyzer performed in this work was used for the determination of the Zn(II) ion in three different pharmaceuticals (Wellzinc-20-20mg Wellona pharma-India, Coral laboratories LId-20mg-India, and Pharma developpement-20mg-France), and was compared with UV-spectrophotometric methods via absorbance measurements recorded at λmax = 227nm. A series of solutions was prepared for each drug, and standard addition procedures were applied, which were then measured in a UV spectrophotometer. The results of the analyses for each of the two methods are summarized in Table 11 with a confidence level of 95% (two-tailed).

In addition to the reported linear range (0.05–18 mmol-1), detection limit (0.489 μg.sample-1) and percentage relative standard deviation (RDS% > 1), Further validation studies have been made to comprehensively evaluate the proposed method. Recovery tests have been applied for different pharmacological dosage forms such as capsules, sustained–release tablets, and syrup. In compliance with the acceptance guideline established by the pharmacopeia, the initial recovery finding is expected to fall between 98–102%. Interference investigations will be carried out using common ions such as Ca + 2, Mg + 2, and Fe^{+3}. Preliminary investigation explained that these ions, at amounts frequently observed in pharmaceuticals, have no significant effect on Zinc determination, confirming the selectivity of the precipitation reaction. Relative standard deviation (RSD%) will be evaluated via repeated measurement within a single day (intra-day RSD% > 2%) and over multiple consecutive days (inter-day RSD% > 3%). The results fall within the limit of the standard pharmacopeia, confirming the acceptable repeatability and reproducibility. Long-term monitoring of the analyzer maintained a stable baseline and constant sensitivity. These additional validations strongly verify that the proposed method was accurate, unaffected by common interferences, stable over time, and reliable for pharmaceutical quality control. As a summary, recovery tests with capsule, sustained release tablets, and syrup verified accuracy (98.7–100.1%). Intra and inter-day

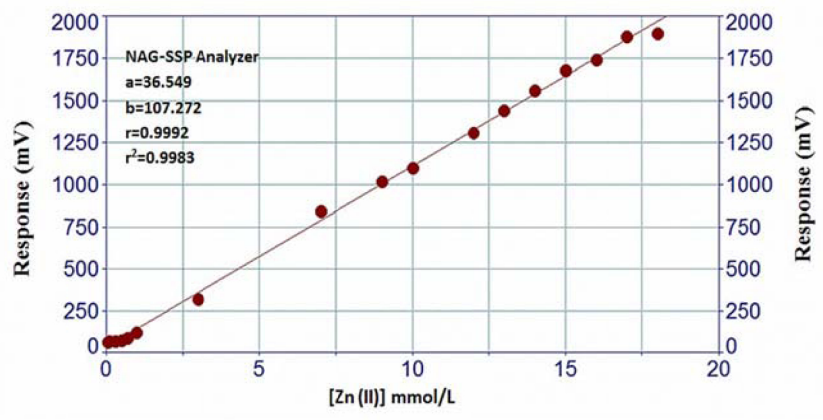

Fig. 12. The calibration curve for the relationship between Zn(II) concentration and turbidimetric measurements.

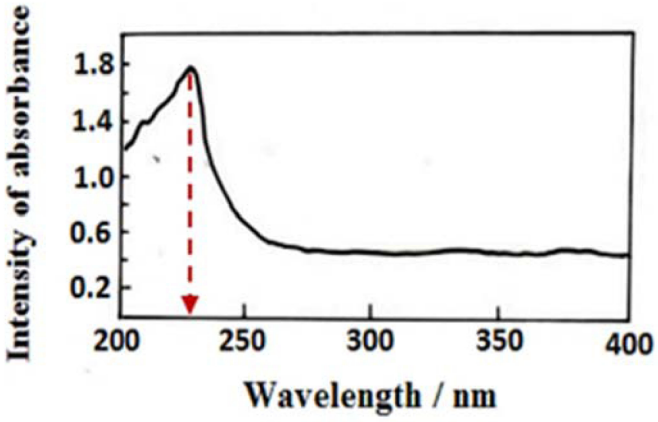

Fig. 13. Absorbance spectrum of the zinc sulfate heptahydrate $ZnSO_4.7H_2O$.

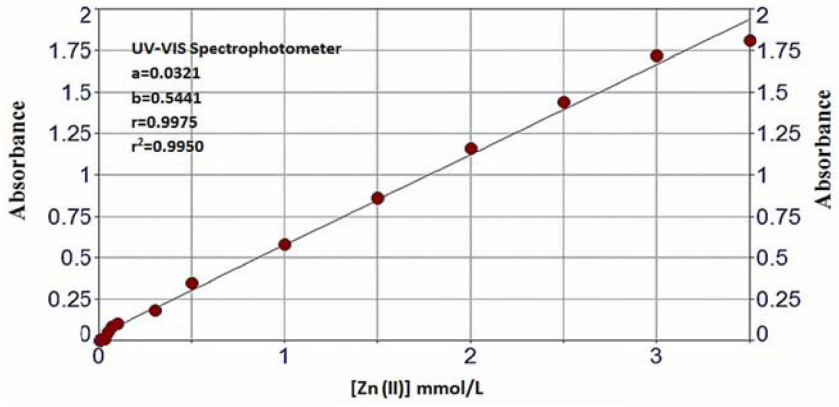

Fig. 14. Calibration plot for the relationship between Zn(II) concentration and spectrophotometric measurements.

precision ranged from (1.1–1.6% RSD) and (1.9–2.6% RSD), respectively, and are all within the acceptable limit of the pharmacopeia. Selectivity was provided via the interferences studied with Ca + 2, Mg + 2, and Fe + 3 up to fivefold excess, giving > 2% signal variation. As conclusion, these results of validation demonstrate that the method was precise, accurate, selective and stable for pharmaceutical quality control.

Variance homogeneity between the two methods was confirmed using Levene's test, which gives ($P < 0.05$), ensuring the validation of the t-test under

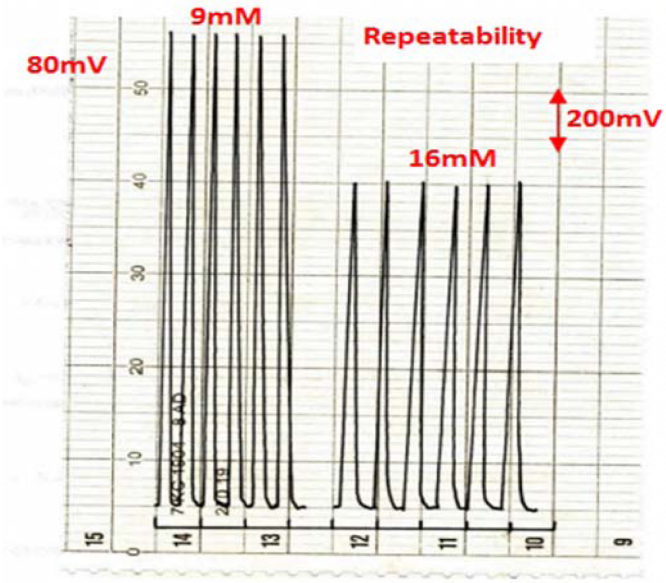

Fig. 15. Repeatability profile for 9 and 16 mmol.L^{-1} concentrations of Zn(II) using the developed turbidimetric instrument.

Table 10. Analytical parameters and calibration equation for UV-Vis spectrophotometer. Comparison between UV-Vis spectrophotometry methods and the NAG-SSP analyzer.

				Detection limit	Repeatability n=6	
Type of mode of range concentration	Range of concentration of Zn(II) mmol.L^{-1}	$\hat{Y}$(mV) = a ± SD + b ± SD[x] mmol.L^{-1}	r r2 R_2 %	Gradual dilution of the minimum concentration	Concentration mmol.L^{-1}	RSD%
Scatter plot	0.008–3.7	0.042 ± 0.021 + 0.523 ± 0.011 [Zn(II)] mmol.L^{-1}	0.9969 0.9939 99.39%	(0.005 mmol.L^{-1})	0.1	0.523
Linear range	0.008–3.5	0.032 ± 0.018 + 0.544 ± 0.011 [Zn(II)] mmol.L^{-1}	0.9975 0.9950 99.50%		3.0	0.325

the assumption of equal variance. Normality of data distribution was evaluated using the Shapiro-Wilk test, and all groups display non–significant deviation from normality ($P < 0.05$). The number of replications (n=6) for each drug and method was selected to attain a statistical power of at least 0.8 at 95% confidence level. This guarantees that the proposed method has enough power to identify significant variance between methods. The comparison between the NAG-SSP analyzer and UV-Vis spectrophotometry is statistically robust and reliable by verifying variance quality, normal distribution, and proper sample size.

Additionally, Table 11 provides information on the Zn(II) ion content for each pharmaceutical, as well as the recovery of determination. An individual and paired t-test was also conducted.

A comparison was made via two statistical treatments: in the first statistical test, a comparison was made between the 20 mg quoted for each pharmaceutical with the mean value of each of their content as determined by the NAG-SSP instrument.

H_o:μ(20mg) = Wi represents the proposed hypothesis

H_o:μ(20mg) ≠ Wi represents the alternative hypothesis

From the results obtained, it was observed that there was no significant difference between the measured mean values (Wi) and the official quoted values (μ 20mg) because t-tab(4.303) was greater than the t-value for these pharmaceuticals.

The second comparison used a paired t-test to compare the results obtained from each method, ignoring which company produced the tablet.

Null hypothesis: H_o:μNAG-SSP instrument = μUV-VIS Spectrophotometer instrument.

Alternative hypothesis: H_1:μNAG-SSP instrument ≠ μUV-VIS Spectrophotometer instrument.

Table 11. Standard procedure results and statistical treatment for the determination of the zinc ion in three pharmaceuticals using the NAG-SSP analyzer and UV-Vis spectrophotometer.

Sample No.	Commercial name content and company country	Standard addition equation at 95% for n-2 $\hat{Y}$(mV) = a ± sat + b ± sbt[Zn(II)] r,r2,R_2%	Practical content Wi±4.303σn-1/$\sqrt{n}$(mg) for (n = 3), at 95%	Recovery%	Individual t-test	Paired t-test between NAG-SSP analyzer with UV-vis spectrophotometer
		Developed Instrument				
		UV-VIS spectrophotometer				
1	Wellzinc-20 20 mg Wellona pharma-India	40.130 ± 1.224 + 163.146 ± 3.241 0.9989, 0.9978, 99.78%	19.681 ± 2.314	98.41%	|−0.593 | <4.303	tcal = 2.215 ttab = 4.303 2.215 <4.303 Sig.2-tailed = 0.270 0.270 >0.05
		0.183 ± 0.0182 + 0.759 ± 0.0221	19.292 ± 2.324	96.46%	|−2.567 | <4.303	
2	Coral laboratories LId 20 mg India	38.823 ± 2.021 + 161.897 ± 3.421 0.9986, 0.9972, 99.72%	19.210 ± 1.323	96.05%	|−0.322 | <4.303	
		0.168 ± 0.0212 + 0.706 ± 0.121	19.063 ± 2.021	95.31%	|−1.312| <4.303	
3	Pharma development 20 mg France	42.321 ± 1.832 + 176.338 ± 3.582 0.9899, 0.9799, 97.99%	19.200 ± 1.832	96.00%	|−1.994 | <4.303	
		0.171 ± 0.0212 + 0.701 + 0.123	19.282 ± 2.321	96.41%	|−1.331| <4.303	

The results obtained, shown in Table 11, column 7, clearly indicate that there was no statistically significant difference between the NAG-SSP instrument and UV-Vis spectrophotometer; however, the developed method allows for rapid analysis at reduced cost at the 95% ($\alpha = 0.05$) confidence level.

Conclusion

This study successfully developed and validated the NAG 5SX1 1D SSP analyzer for the determination of zinc ions in pharmaceutical formulations. The suggested method successfully approaches the research objective of providing a highly sensitive, portable, and affordable substitute for conventional spectrophotometric methods. The analyzer exhibited a low limit of detection (0.489 $\mu g \cdot$ sampl-1), a wide range of linearity (0.05–18 mmol·L^{-1}), outstanding precision with RSD% >1, and minimum sensitivity to electronic noise. Innovative design factors such as varied internal tube width and regulated multi-LED light are significantly responsible for performance quality. The current method offers easier operation, cheaper, and better portability for routine quality control compared to the conventional UV-Vis spectrophotometric method. Despite the benefit, the current technique is limited by the need for mercuric chloride, thereby calling for careful security measures and environmentally responsible waste management. Future research will focus on the analyzer capabilities to determine other metal ions and assess its suitability for the determination of zinc ions in biological samples.

Overall, the proposed work demonstrates the practical utility and scientific significance of the developed analytical approach in pharmaceutical analysis. By directly aligning experimental findings with the study objectives, emphasizing both limitations and strengths, and offering distinct future directions.

Acknowledgements

The authors would like to thank Prof. Dr. Issam M. A. Shakir Al Hashimi for his support in manufacturing the analyzer.

Authors' declaration

- Conflicts of Interest: None.
- We hereby confirm that all the Figures and Tables in the manuscript are ours. Furthermore, any Figures and images that are not ours have been included with the necessary permission for republication, which is attached to the manuscript.
- No animal studies are present in the manuscript
- No human studies are present in the manuscript.

- Ethical Clearance: The project was approved by the local ethical committee at the University of Kerbala.

Authors' contributions statement

R. S. H.: wrote the manuscript. M. A. K. Al: Performed the experiment in its chemical parts and wrote the manuscript. N. Sh. T: Proposed the idea of the research and support for the manufacturing of the NAG-SSP analyzer. I. M. Sh: wrote the manuscript and explained the interpretation. All the authors have read and approved the final version for publication.

References

1. Ingalls WR. Production and properties of zinc: A treatise on the occurrence and distribution of zinc ore, the commercial and technical conditions affecting the production of the spelter, its chemical and physical properties and uses in the arts, together with a historical and statistical review of the industry. 1902.
2. Rink L. Zinc and the immune system. Proc Nutr Soc. 2007;59(4):541–52 https://doi.org/10.1017/S0029665100000781.
3. Hojyo S, Fukada TJJoir. Roles of zinc signaling in the immune system. J Immunol Res. 2016;2016(1):6762343. https://doi.org/10.1155/2016/6762343.
4. Tesfaye E, Chandravanshi BS, Negash N, Tessema M. Electrochemical determination of zinc (II) using N1-hydroxy-N1, N2-diphenylbenzamidine and multi-walled carbon nanotubes modified carbon paste electrode. Heliyon. 2023;9(6). https://doi.org/10.1016/j.heliyon.2023.e17346.
5. Dinçer R, Karabiberoğlu ŞU, Dursun Z. Simultaneous electrochemical determination of trace zinc (II), cadmium (II) and lead (II) in lipsticks using a novel electrode covered with bismuth/over-oxidized poly (xylenol blue) film. Microchem J. 2023;189:108548. https://doi.org/10.1016/j.microc.2023.108548.
6. Zhou F, Li C, Zhu H, Li Y. A novel method for simultaneous determination of zinc, nickel, cobalt and copper based on UV–vis spectrometry. Optik. 2019;182:58–64. https://doi.org/10.1016/j.ijleo.2018.12.159.
7. Zvěřina O, Vychytilová M, Rieger J, Goessler W. Fast and simultaneous determination of zinc and iron using HR-CS GF-AAS in vegetables and plant material. Spectrochimica Acta Part B: Atomic Spectroscopy. 2023;201:106616. https://doi.org/10.1016/j.sab.2023.106616.
8. Kagaya S, Hida-Matsuda K, Tsuzaka S, Minami C, Gemmei-Ide M, Cattrall RW, *et al.* The determination of zinc using flow injection and continuous flow analysis combined with a polymer inclusion film-coated column: Application to the determination of zinc in alloys and commercial lithium chloride. Talanta. 2023;259:124545. https://doi.org/10.1016/j.talanta.2023.124545.
9. Al-Saadi KHI, Al-Awadie NST. CFIA-ISNAG fluorimeter for the determination of bromhexine-HCl in drugs via the measurement scattered light at±90. Iraqi J Sci. 2023:5476–90. https://doi.org/10.24996/ijs.2023.64.11.2.
10. Cerda V, Ferrer L, Portugal LA, de Souza CT, Ferreira SL. Multisyringe flow injection analysis in spectroanalytical techniques–A review. TrAC, Trends Anal Chem. 2018;98:1–18. https://doi.org/10.1016/j.trac.2017.10.016.
11. Mohammed BS, Turkey NS. New homemade NAG-4SX3-3D analyzer for quantification of cyproheptadine hydrochloride by its precipitating with calcium hexacyanoferrate. J Chemical Papers. 2024;78(2):1277–90. https://doi.org/10.1007/s11696-023-03165-9.
12. Jasim AN, Turkey NS, Abd-Alrazack HF. Design a continuous microfluidic flow cell for turbidimetric-flow injection technology: A new approach for routine analysis of active pharmaceutical formulations. Anal Methods Environ Chem J. 2022;5(02):90–104. https://doi.org/10.24200/amecj.v5.i02.184.
13. Shakir IM, Mohammed BS, Turkey NS. A novel study in the determination of loratadine in pharmaceutical samples by precipitating with 3, 5-dinitrosalicylic acid utilizing the NAG_4SX3_3D analyzer at 0-180o in conjunction with the continuous flow injection analysis (CFIA) technique. Adv J Chem A. 2024;7:260–77. https://doi.org/10.48309/AJCA.2024.429274.1462.
14. Saurina J, Hernández-Cassou SJAca. Quantitative determinations in conventional flow injection analysis based on different chemometric calibration statregies: A review. Anal Chim Acta. 2001;438(1–2):335–52. https://doi.org/10.1016/S0003-2670(01)00862-5.
15. Tzanavaras PD, Themelis DGJAca. Review of recent applications of flow injection spectrophotometry to pharmaceutical analysis. Anal Chim Acta. 2007;588(1):1–9. https://doi.org/10.1016/j.aca.2007.01.060.
16. Chen X, Yin G, Zhao N, Gan T, Yang R, Xia M, *et al.* Simultaneous determination of nitrate, chemical oxygen demand and turbidity in water based on UV–Vis absorption spectrometry combined with interval analysis. Spectrochimica Acta Part A: Molecular and Biomolecular Spectroscopy. 2021;244:118827. https://doi.org/10.1016/j.saa.2020.118827.
17. A Kadhim Al-Banaa M, Turkey NS, Jasim ANJA, Research BC. Calcium hexacyanoferrate (II) as a precipitating reagent for the determination of mebeverine using multiple flow cells with summed (S/N) responses in NAG-4SX3-3D instrument. Anal Bioanal Chem Res. 2024;11(2):239–45. https://doi.org/10.22036/abcr.2024.435208.2032.
18. Turkey AL-A, Wadie NS, Saleem AJ. New turbidimetric method for determination of ketotifen fumarate in pharmaceutical drugs by using line-continuous flow injection manifold design of KTF-Ammonium molybdate (Am) system. Int J Pharm Sci Res. 2020;12(2). https://doi.org/10.31838/ijpr/2020.12.02.0046.
19. Mezaal EN. New method for the evaluation of propranolol with phosphotungstic acidvialong distance chasing photometer (NAG-ADF-300-2) using continuous flow injection analysis. Int J Pharm Sci Res. 2019;11(4). https://doi.org/10.31838/ijpr/2019.11.04.008.

تحليل الحقن الجرياني المستمر شبه الالي – تقدير التعكيرية للزنك في مستخصرات الادوية

رغد سعد حاتم [1] ، مروة عبد الرضا كاظم [2] ، نغم شاكر تركي[3] ، احسان مهدي شهيد[4]

[1]قسم علوم الحياة , كلية العلوم , جامعة كربلاء , كربلاء , العراق.
[2]قسم الأدلة الجنائية, كلية العلوم , جامعة الكرخ للعلوم , بغداد , العراق.
[3]قسم الكيمياء, كلية العلوم , جامعة بغداد , بغداد , العراق.
[4]قسم الكيمياء, كلية العلوم , جامعة كربلاء, كربلاء, العراق.

الخلاصة

قيمت هذه الدراسة التقنية الحديثة المطورة لجهاز التحليل المصنع داخليا NAG-5SX1-1D-SSP وذلك باستخدام التفاعل المعتمد لأيون الزنك (II) مع ثايوسيانات الامونيوم وكلوريد الزئبق (II) لإنتاج راسب ابيض. التعكيرية تم قياسها من خلال انعكاس الضوء الساقط الذي يصطدم بالجزيئات المترسبة على السطح عند درجة 0-180 باستخدام هذا الكاشف. شمل التقييم تحديد المدى الخطي، حد الكشف، ونسبة الانحراف القياسي النسبي للتكرار حيث بلغت القيم 0.05-18 ملي مول / لتر، 0.489 مايكروكرام / نموذج واقل من 1% فيما يتعلق بتفاعل ايون الزنك (II) في المستحضرات الصيدلانية. اكدت هذه النتائج موثوقية وقوة الجهاز المطور لتقدير الزنك الثنائي في المستحضرات الصيدلانية. وقد اثبت تطبيق أسلوب الاضافة القياسية نجاحه في الكشف عن ايون الزنك في ثلاثة ادوية. اجري تحليل مقارن بين الجهاز المبتكر حديثا والطريقة التقليدية (مطياف الاشعة فوق البنفسجية – المرئية) عند طول موجي 227 نانوميتر وذلك بتطبيق اختبار t الفردي والمزدوج. خضعت البيانات المستحصلة لمعالجة رياضية دقيقة ولم يظهر أي تباين يذكر بين الطريقتين في تحليل ثلاثة ادوية مختلفة عند حدود ثقة 95%.

الكلمات المفتاحية: تحليل الحقن التدفقية، أيون الزنك (II)، العكارة، ثيوسيانات الزئبق (II)، التحليل الصيدلانية.